

Improved extraction of hydrologic information from geophysical data through coupled hydrogeophysical inversion

A. C. Hinnell,¹ T. P. A. Ferré,¹ J. A. Vrugt,^{2,3} J. A. Huisman,⁴ S. Moysey,⁵ J. Rings,⁴ and M. B. Kowalsky⁶

Received 1 April 2008; revised 6 October 2009; accepted 27 October 2009; published 9 April 2010.

[1] There is increasing interest in the use of multiple measurement types, including indirect (geophysical) methods, to constrain hydrologic interpretations. To date, most examples integrating geophysical measurements in hydrology have followed a three-step, uncoupled inverse approach. This approach begins with independent geophysical inversion to infer the spatial and/or temporal distribution of a geophysical property (e.g., electrical conductivity). The geophysical property is then converted to a hydrologic property (e.g., water content) through a petrophysical relation. The inferred hydrologic property is then used either independently or together with direct hydrologic observations to constrain a hydrologic inversion. We present an alternative approach, coupled inversion, which relies on direct coupling of hydrologic models and geophysical models during inversion. We compare the abilities of coupled and uncoupled inversion using a synthetic example where surface-based electrical conductivity surveys are used to monitor one-dimensional infiltration and redistribution. Through this illustrative example, we show that the coupled approach can provide significant reductions in uncertainty for hydrologic properties and associated predictions if the underlying model is a faithful representation of the hydrologic processes. However, if the hydrologic model exhibits structural errors, the coupled inversion may not improve the hydrologic interpretation. Despite this limitation, our results support the use of coupled hydrogeophysical inversion both for the direct benefits of reduced errors during inversion and because of the secondary benefits that accrue because of the extensive communication and sharing of data necessary to produce a coupled model, which will likely lead to more thoughtful use of geophysical data in hydrologic studies.

Citation: Hinnell, A. C., T. P. A. Ferré, J. A. Vrugt, J. A. Huisman, S. Moysey, J. Rings, and M. B. Kowalsky (2010), Improved extraction of hydrologic information from geophysical data through coupled hydrogeophysical inversion, *Water Resour. Res.*, **46**, W00D40, doi:10.1029/2008WR007060.

1. Introduction

[2] Quantitative subsurface hydrologic analysis is based on the conceptualization, development, and testing of hydrologic models [Neuman *et al.*, 2003]. Model conceptualization is the process of observing a system and proposing a simplified representation of the system that incorporates the features deemed important to the processes under observa-

tion (e.g., water flow or solute transport). Model development translates the proposed conceptual model (or models) to a mathematical or numerical model(s) that can be used to test a hydrologic hypothesis. Model testing is an analytical process, wherein the predictions of the model(s) are compared quantitatively with the available data. The goals of model testing are to find the values of the adjustable parameters in a model that result in the best fit of the model predictions to the data (calibration) [e.g., Kim *et al.*, 1999; Poeter and Hill, 1999, Vrugt *et al.*, 2009b]; to quantify the goodness of fit and assess parameter nonuniqueness for the calibrated model [e.g., Vrugt *et al.*, 2003; Mugunthan and Shoemaker, 2006]; and, increasingly, to compare the goodness of fit of multiple models to the data [Neuman, 2003; Ye *et al.*, 2004; Trolldborg *et al.*, 2007, Vrugt and Robinson, 2007]. The results of model testing can be used to revise model conceptualization and/or development as well as to guide the design of future data collection activities. In short, the three phases of model-based hydrologic analysis can be described as (1) hypothesizing which subsurface structures and processes are significant, (2) trans-

¹Hydrology and Water Resources, University of Arizona, Tucson, Arizona, USA.

²Center for Nonlinear Studies, Los Alamos, New Mexico, USA.

³Department of Civil and Environmental Engineering, Henri Samueli School of Engineering, University of California, Irvine, California, USA.

⁴ICG 4 Agrosphere, Forschungszentrum Jülich, Jülich, Germany.

⁵Environmental Engineering and Earth Sciences, Clemson University, Clemson, South Carolina, USA.

⁶Earth Sciences Division, Lawrence Berkeley National Laboratory, Berkeley, California, USA.

lating this hypothesis into mathematical expressions and parameterizations, and (3) testing the hydrologic models against observations.

[3] To test multiple conceptual or mathematical models effectively, the inverse approach used for parameter calibration must be efficient in extracting relevant information from the observed data. The efficiency of parameter calibration depends on both the inverse algorithm selected and the way in which the inverse problem is posed. Inverse analysis is common to most scientific disciplines. Hydrologic science has adopted and developed many inverse approaches. But, until recently, there have been few studies regarding the formulation of efficient inversion strategies that incorporate multiple measurement types, including indirect measurements. The development of such inversion strategies for hydrologic problems is critical as the use of geophysical methods becomes increasingly common for monitoring subsurface flow and transport.

[4] Geophysics is a mature discipline that has made fundamental contributions to a range of scientific disciplines [e.g., *National Academy of Sciences*, 2000]. Many of these contributions stem from the ability of geophysical methods to provide unparalleled views into the earth. As a result, geophysics is a cornerstone of oil and mineral exploration and production. Increasingly, geophysical imaging of the subsurface is also being used to conceptualize and develop hydrologic models through mapping subsurface structures and improving estimates of the spatial distribution of hydrologic properties [e.g., *Hubbard and Rubin*, 2000; *Vereecken et al.*, 2004]. Advanced joint inversion methods have been developed to use multiple geophysical methods to reduce the nonuniqueness of the estimated structural models [e.g., *Vozoff and Jupp*, 1975; *Gallardo and Meju*, 2003, 2004; *Linde et al.*, 2006a]. In addition, geostatistical methods have been developed to estimate hydrologic property distributions based on statistical correlations present in geophysical images [e.g., *Cassiani et al.*, 1998; *Hubbard et al.*, 1999; *Yeh et al.*, 2002; *Chen et al.*, 2004]. Finally, hydrologic structure and parameter distributions have been estimated simultaneously using geophysical and hydrologic data [e.g., *Hyndman et al.*, 1994; *Hyndman and Gorelick*, 1996; *Chen et al.*, 2006; *Linde et al.*, 2006b]. In general, there is wide and growing recognition of the value of geophysics for subsurface imaging to aid in the conceptualization of hydrologic models.

[5] The use of geophysical data for testing hydrologic models also has a long history. For example, many studies have used electrical [e.g., *Daily et al.*, 1992; *Park*, 1998; *Kemna et al.*, 2002; *Sandberg et al.*, 2002; *French and Binley*, 2004; *Halihan et al.*, 2005; *Vanderborght et al.*, 2005; *Cassiani et al.*, 2006; *Chambers et al.*, 2006] and/or electromagnetic [e.g., *Binley et al.*, 2001; *Day-Lewis et al.*, 2003; *Cassiani et al.*, 2004; *Lambot et al.*, 2004; *Turesson*, 2006; *Deiana et al.*, 2008; *Looms et al.*, 2008b] methods to monitor changes in water content or solute concentration with time. Despite the differences in hydrologic targets and geophysical methods used in these studies, they have all followed the sequential approach to using the geophysical data to test a hydrologic model outlined in Figure 1a, which we refer to as uncoupled hydrogeophysical inversion. Uncoupled hydrogeophysical inversion follows three independent steps.

[6] 1. Geophysical survey data are inverted to estimate the spatial distribution of a geophysical property throughout the subsurface region of interest (Figure 1a, geophysical inversion).

[7] 2. A petrophysical relation [e.g., *Archie*, 1942; *Topp et al.*, 1980; *Binley et al.*, 2005] is used to convert the geophysical property map[s] to hydrologic state distributions at each measurement time (Figure 1a, dashed line linking geophysical inversion to hydrologic inversion).

[8] 3. The inferred hydrologic states are used either independently or together with directly measured hydrologic states to test hydrologic models (Figure 1a, hydrologic inversion).

[9] The gray process boxes in Figure 1a are present to illustrate how multiple data streams could be included in the uncoupled analysis. In the examples presented here, only one data stream (electrical conductivity data) is used. This approach, using a single data stream, is illustrated by the black process boxes.

[10] Uncoupled inversion propagates measurement errors and uncertainties related to parameter resolution and uniqueness that arise during the independent inversion of the geophysical data to the hydrologic analysis through the petrophysical relation. A particular issue stems from the fact that geophysical imaging typically requires a large number of parameters to retain the flexibility necessary to capture arbitrary, complex distributions of properties in the subsurface (e.g., the electrical conductivity distribution associated with a contaminant plume). As a result, geophysical inverse procedures commonly require the use of prior information (e.g., a smoothness constraint) to stabilize underconstrained problems [e.g., *Menke*, 1984]. It has been recognized that this regularization may not reflect the hydrologic conditions and can limit the value of hydraulic property estimates derived from geophysical observations [*Day-Lewis et al.*, 2005; *Chen et al.*, 2006; *Slater*, 2007].

[11] There have been several alternatives proposed to improve the uncoupled inversion approach. The petrophysical conversion can be improved using apparent calibration relationships that vary with location to compensate for the impacts of the spatially variable sensitivity of measurement methods and associated inversion artifacts [e.g., *Moysey et al.*, 2005; *Singha and Moysey*, 2006]. In addition, temporal relaxation techniques can be used in the geophysical inversion to interpret multiple time slices simultaneously, thereby effectively reducing the number of free parameters to be estimated [*Day-Lewis et al.*, 2002]. Finally, some joint inversion approaches allow for simultaneous determination of geophysical property distributions and petrophysical relations [e.g., *Hyndman et al.*, 1994; *Hyndman and Gorelick*, 1996; *Chen et al.*, 2006; *Linde et al.*, 2006b]. However, all of these proposed advances still rely on an independent geophysical inversion step to infer hydrologic states.

[12] We examine an alternative approach to uncoupled hydrogeophysical inversion for model testing. The approach, hereafter referred to as coupled hydrogeophysical inversion [*Ferré et al.*, 2009], is based on the premise that the goal of model testing is to determine the degree of consistency between a proposed hydrologic model and associated observations, thereby assessing the likely validity of a proposed hydrologic model. From this basis, it seems most reasonable that the geophysical data should be interpreted in the context of the proposed hydrologic model. This differs

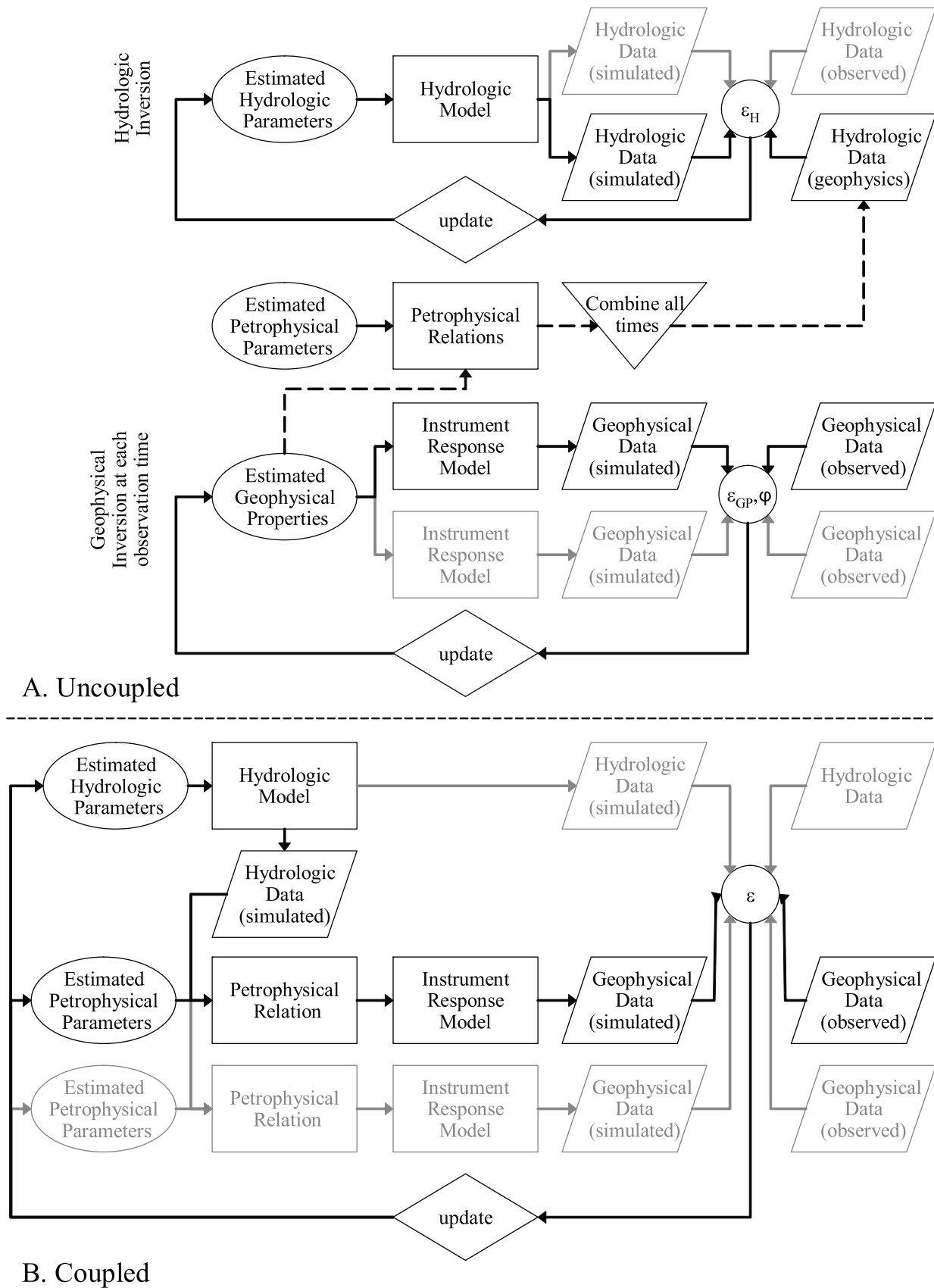


Figure 1. Analysis flowcharts for (a) uncoupled and (b) coupled integration of geophysical data in hydrologic analysis. Grey boxes in the flowcharts show additional data sources that could be included but are not used in our example. Note that each sequence of petrophysical relation, instrument response model, and geophysical data (simulated) in the coupled and uncoupled approaches represents a different measurement type.

from the joint inversion approaches outlined previously. In the joint approaches, a relationship between hydrologic and geophysical (or between two geophysical) properties is assumed, but the hydrologic model is not used to guide the geophysical interpretation [Ferré *et al.*, 2009].

[13] The workflow of coupled inversion, shown in Figure 1b, is similar to that used by Rucker and Ferré [2004] and Kowalsky *et al.* [2005], which was summarized by Ferré *et al.* [2009]. It is typical of nonlinear optimization problems where an initial parameter set is proposed, used to simulate observed measurements, and then updated based on misfit between the simulated and observed data values. The distinguishing factor in the coupled inversion strategy is that, for any observed geophysical data set, we couple a hydrologic and geophysical model to represent the forward model in the optimization. In practice, this is achieved through a straightforward and flexible process where an initial set of hydraulic parameters is proposed and a forward hydrologic model (e.g., flow and reactive transport) is run using these parameter values. The model-predicted hydrologic states (e.g., water content) are converted to geophysical properties using petrophysical relations. The resulting geophysical property distributions are used to predict the response for each measurement method at each observation time and location using geophysical (forward) models. During inversion, the hydraulic properties and the petrophysical model parameter values are optimized to minimize the difference between predicted and measured geophysical observations. In Figure 1b, the gray process boxes illustrate how the coupled inversion approach could use multiple data streams. In the examples presented here, only one data stream (electrical conductivity) is used as illustrated by the black process boxes.

[14] The coupled and uncoupled approaches to inversion have several distinct, yet important differences that can impact both the computational effort and the uniqueness of the interpretations. Coupled inversion does not require a geophysical imaging step, thereby avoiding geophysical resolution problems related to the estimation of a large number of poorly constrained parameters. This alleviates the need to construct point-specific apparent calibration relationships to account for the effects of the spatially variable measurement sensitivity [Moysey *et al.*, 2006]. This is especially important when the spatial sensitivity of the geophysical method depends on the spatial distribution of the hydrologic state of interest [Klenke and Flint, 1991; Ferré *et al.*, 1996; Furman *et al.*, 2003]. Another advantage is that explicit assumptions regarding the spatial continuity of geophysical properties (e.g., smoothness) are no longer required to stabilize the geophysical component of the inverse problem because the hydrologic model defines the spatial arrangement of geophysical properties using physically based predictions of the hydrologic properties. Temporal regularization methods are also no longer required because the temporal dynamics are also enforced by the physics underlying the hydrologic model. Furthermore, because the underlying hydraulic properties are estimated directly, there is no need to consider joint inverse techniques explicitly. Rather, all of the data are considered in a single inversion and any of the correlations among measurement types that form the basis of joint inversion techniques (e.g., cross gradients in work by Gallardo and Meju [2004]) arise naturally by coupling the process model (i.e., the hydrologic model) and the geophysical models. In summary, because coupled

inversion interprets the geophysical data in the context of the proposed hydrologic model, it provides a better test of the consistency of the proposed hydrologic model with the geophysical observations.

[15] Despite the potential advantages of coupled inversion, relatively few investigators have used this method to constrain hydrologic models with geophysical data [Rucker and Ferré, 2004; Kowalsky *et al.*, 2004, 2005, 2009; Sicilia and Moysey, 2007; Finsterle and Kowalsky, 2008; Looms *et al.*, 2008a; Lehtikoinen *et al.*, 2009]. None of these investigations has directly compared coupled and uncoupled approaches for model testing.

[16] In this study, we demonstrate the advantages and limitations of coupled hydrogeophysical inversion using an illustrative example of infiltration into the unsaturated zone monitored by electrical conductivity surveys. We use a synthetic example with known hydrologic and petrophysical properties to allow for a quantitative comparison of the accuracy of uncoupled and coupled hydrogeophysical inversion approaches. This relatively simple example allows us to isolate the effects of coupled and uncoupled inversion from complications arising from soil and petrophysical parameter heterogeneity, boundary condition uncertainty, and model structural error. In particular, we examine the impacts of structural errors in the model on hydrogeophysical inversion by comparing inversions performed with two different data sets. The first data set is based on the analytical infiltration model of Philip [1957], which assumes a homogeneous soil. The second data set is generated using a numerical model for unsaturated flow in a heterogeneous medium (HYDRUS 1D) [Simunek *et al.*, 1999]. The homogeneous model is used for the inversion of both data sets, thereby introducing model structural errors for the case where the subsurface is actually heterogeneous. This latter analysis is intended to represent the common practice of applying hydrologic models and parameter distributions that are considerably simpler than reality to make numerical inversion tractable.

2. Problem Statement

[17] Our objective is to compare the performance of coupled and uncoupled hydrogeophysical inversion. We examine the ability of each approach to constrain soil properties during an infiltration event in a homogeneous soil. In addition, we present an example to assess whether the inversion results are affected by the introduction of model structural errors.

[18] The specific problem we consider is the use of electrical conductivity to monitor the advance of a wetting front during one-dimensional infiltration under a zero-ponding depth boundary condition at the ground surface into a porous medium with uniform initial pressure head. After 5 days of infiltration, the monitoring of water redistribution with electrical conductivity continues for an additional 15 days with a zero-flux boundary condition maintained at the ground surface. The geophysical data consisted of a time series of measurements made with multiple electrical conductivity arrays located at the ground surface. The arrays have a common midpoint that is centered in the infiltration area. We use these arrays to monitor one-dimensional water flow with the assumption that flow is predominantly vertical and that the infiltration area is large compared to the max-

imum electrode separation. For the maximum current electrode separation considered (45 m), the synthetic system could represent an artificial recharge facility or an ephemeral stream or a lake. However, the entire system (depth of wetting front, electrode separations, scale of lateral heterogeneity, and measurement time interval) could be scaled down or scaled up without loss of generality.

[19] In the work presented herein, we consider two flow systems with differing levels of complexity. We first examine infiltration into a homogeneous soil profile, followed by a case study considering infiltration into a heterogeneous soil profile comprising different horizontal layers. Two approaches to modeling these different flow systems are considered: (1) analytical models of water and electrical flow in homogeneous soils and (2) numerical models capable of accurately representing water and electrical flow in heterogeneous soils. These coupled hydrologic and geophysical models are hereafter referred to as the analytical and numerical models, respectively. The analytical models provide a somewhat crude approximation of the actual flow processes occurring in a heterogeneous material, yet have the advantage of being computationally efficient. This is a significant practical benefit, and we therefore explore whether the use of models that fail to consider the detail of the hydrologic system (e.g., heterogeneity) can provide accurate results using coupled hydrogeophysical inversion.

2.1. Solution of the Forward Problem Using a Numerical Model

[20] The coupled hydrogeophysical inverse problem requires three different forward models: a hydrologic model, a geophysical model (electrical conductivity for a given electrode array), and a petrophysical relation. The hydrologic model enables the simulation of water content with depth and time based on a numerical solution of Richards' equation. The geophysical model simulates electrical conductivities that would be measured for each electrode array. This is achieved through a numerical solution for electrical flow with the electrical conductivity distribution (which depends on the water content profile calculated with the hydrologic model) at a given time. To form realistic electrical conductivity measurements in the case studies considered herein, we added synthetic measurement error to the error-free electrical conductivities simulated with the geophysical model. The procedure for solving the hydrogeophysical problem with a highly accurate numerical solution is described in this section. In section 2.2, a simplified, and hence more computationally efficient hydrogeophysical approach is given using an analytical model.

2.1.1. Hydrologic Model

[21] The hydrologic problem that we consider is infiltration and drainage in a vertically heterogeneous soil profile. One-dimensional water flow is described by Richards' equation

$$\frac{\partial}{\partial z} \left(K(\psi) \left(\frac{\partial \psi}{\partial z} + 1 \right) \right) = \frac{\partial \theta}{\partial t}. \quad (1)$$

In equation (1), ψ [L] is the pressure head, θ [-] is the volumetric water content, $K(\psi)$ [L T⁻¹] is the hydraulic conductivity (which is a function of the pressure head), z [L]

is the vertical space coordinate (positive upward) and t [T] is time. Equation (1) is solved numerically using a Picard iteration scheme subject to the following boundary and initial conditions:

$$\psi(0, t) = 0 \quad t \leq 120h \quad \frac{\partial \psi}{\partial x}(0, t) = 0 \quad t > 120h \quad (2a)$$

$$\frac{\partial \psi}{\partial x}(z_{\min}, t) = 1 \quad (2b)$$

$$\psi(z, 0) = \psi_n, \quad (2c)$$

where z_{\min} is the depth of the soil profile ($z_{\min} = 15$ m) and ψ_n is the initial pressure head ($\psi_n = -3.05$ m, a value proposed for field capacity by Hillel [1998]). The hydraulic conductivity is defined using the van Genuchten–Mualem model [Mualem, 1976; van Genuchten, 1980]

$$K(\psi) = \begin{cases} K_s \Theta^{0.5} \left(1 - \left(1 - \Theta_m^{\frac{1}{m}} \right)^m \right)^2 & \psi < 0 \\ K_s & \psi \geq 0, \end{cases} \quad (3a)$$

where

$$\Theta(\psi) = \frac{\theta - \theta_r}{\theta_s - \theta_r} = (1 + |\alpha \psi|^n)^{-m} \quad \text{and} \quad m = 1 - \frac{1}{n}. \quad (3b)$$

In equations (3a) and (3b), $\Theta(\psi)$ [-] is the water saturation, K_s [L T⁻¹] denotes the saturated hydraulic conductivity, α [L⁻¹] and n [-] are soil-specific parameters that control the shape of the soil moisture retention function, $\Theta(\psi)$, and θ_r [-] and θ_s [-] are the residual and saturated volumetric water contents, respectively.

[22] The hydrologic simulations are completed using HYDRUS 1D [Simunek *et al.*, 1999]. The model domain is 15 m deep and is composed of 1001 nodes. Heterogeneity is simulated by a random distribution of saturated hydraulic conductivity (Figure 2a) generated with a mean $\log K_s$ of -0.5 [m h⁻¹], variance of 1 and associated correlation length of 0.1 m. The water retention curve parameters (van Genuchten α and n) and the residual and saturated water content (θ_r and θ_s) are assumed uniform throughout the soil profile. Parameter values correspond to a loam soil ($\alpha = 3.6$ m⁻¹, $n = 1.56$, $\theta_r = 0.078$, and $\theta_s = 0.43$) [Carsel and Parrish, 1988]. At the uniform initial pressure head of -3.05 m the initial water content, θ_i , is 0.17 cm³ cm⁻³ and uniform throughout the soil profile.

[23] The water content profile during 5 days of infiltration and 15 days of redistribution are presented in Figure 2b. Black lines show the water content profile at select times during infiltration ($t = \{0, 6, 48, 120\}$ h) and gray lines show the water content profile at select times during redistribution ($t = \{144, 240, 480\}$ h). The depth to the wetting front as a function of time is presented in Figure 3 (diamonds).

2.1.2. Electrical Conductivity Model

[24] We numerically simulate three-dimensional electrical current flow between a dipole in a heterogeneous half-space. Taking advantage of symmetry and the principle of superposition, we solve Poisson's equation for the distribution of electrical potential (V) in cylindrical coordinates

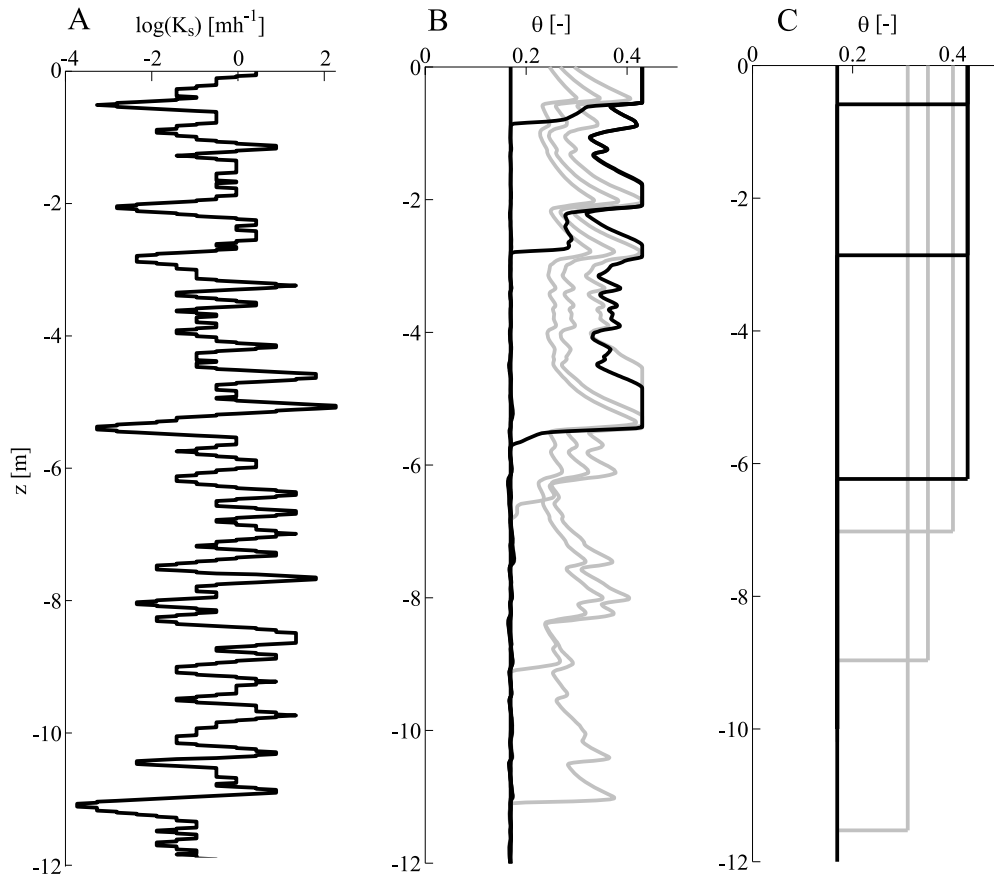


Figure 2. Comparison of two hydrologic models: (1) numerical model (solution to the Richards equation for a heterogeneous soil profile) and (2) analytical model (Philip infiltration and Jury-Horton rectangular drainage) for a homogeneous soil profile. The parameters in the analytical model were estimated using DREAM to get a depth to wetting front behavior similar to the heterogeneous numerical model. (a) Heterogeneous layered saturated hydraulic conductivity. (b) Water content profile with depth for the numerical model at a subset of observation times. Black lines are infiltration phase ($t = 0, 6, 48, 120$ h), and gray lines are redistribution phase ($t = 144, 240, 480$ h). (c) Water content profile with depth for the analytical model at a subset of observation times. Black lines are infiltration phase ($t = 0, 6, 48, 120$ h), and gray lines are redistribution phase ($t = 144, 240, 480$ h).

(where r is the radial direction and z represents the vertical direction) with a vertical variation in the electrical conductivity (σ [S m^{-1}]) associated with the changing water content with depth at an observation time:

$$\frac{1}{r} \frac{\partial}{\partial r} \left(r \sigma(z) \frac{\partial V}{\partial r} \right) + \frac{\partial}{\partial z} \left(\sigma(z) \frac{\partial V}{\partial z} \right) = q(r, z). \quad (4)$$

We use the following boundary conditions:

$$\frac{\partial V}{\partial r}(r_{\max}, z) = 0 \quad \frac{\partial V}{\partial z}(r, 0) = 0 \quad \frac{\partial V}{\partial z}(r, z_{\max}) = 0 \quad q(0, 0) = I_c. \quad (5)$$

In equations (4) and (5) q denotes the source (current electrode) with a corresponding strength of I_c . The numerical electrical flow model was constructed using Comsol Multiphysics (Comsol, Inc., Los Angeles). The 2-D axisymmetric model solves a domain of 150 m by 150 m and is composed of 107529 elements. The size of the model domain and density of finite elements was dictated by

minimizing the influence of the boundary conditions on the simulated voltage in the vicinity of the current electrode (~ 30 m radius from the electrode).

2.1.3. Petrophysical Relation

[25] The hydrologic and electrical conductivity models are linked by the dependence of the soil electrical conductivity on the soil water content. A simple power law relation is used to relate volumetric soil water content and electrical conductivity [Archie, 1942],

$$\sigma(z, t) = a \theta(z, t)^b, \quad (6)$$

where a [S m^{-1}] and b [–] are empirical shape factors that need to be determined through calibration.

[26] In solving the coupled hydrogeophysical inversion, the electrical conductivity model needs to be computed for every observation time using the corresponding water content profile (and petrophysical relation). Unfortunately, even for the relatively simple conditions considered herein, run times are significant. For instance, a single forward

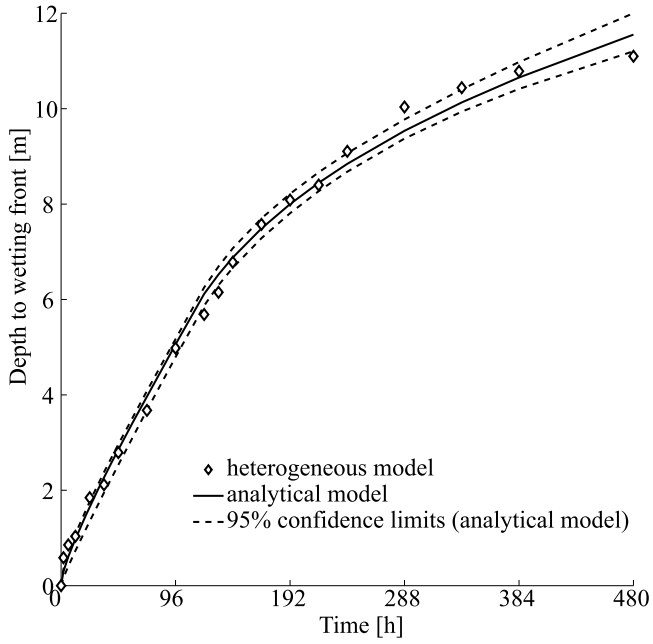


Figure 3. Comparison of the depths of wetting front as a function of time. Diamonds show depth to wetting front for the numerical (heterogeneous) model. The solid line shows depth to wetting front for the analytical model, and the associated 95% prediction limits of the analytical model are defined by the dashed lines.

simulation using the coupled numerical models described above is on the order of 10 min on a desk top computer (dual core 2.66 GHz processor with 4 GB memory). This poses problems for Monte Carlo based sampling methods that generally require many thousands of forward runs to find good parameter solutions. Therefore, we examine whether the approach can be used successfully with a computationally more efficient approximate solution for the hydrologic model. Another possibility is to use high performance computing with multiple computers running in parallel [Huisman *et al.*, 2010]. Yet, such approach limits widespread application and use of the hydrogeophysical inversion framework proposed herein.

2.2. Solution of the Forward Problem Using the Analytical Model

[27] To develop a simplified model of unsaturated flow amenable to Monte Carlo analysis we follow the three phases of a hydrologic analysis that we described earlier, i.e., (1) hypothesis of a conceptual model capturing relevant processes, (2) development of a mathematical model, and (3) testing of the model against observed data. First, we hypothesize that the change in mean moisture content across the wetting front is more significant for affecting the advance of the front than the local fluctuations caused by layered heterogeneity. Specifically, we consider an analytical solution that quantifies the depth of a step wetting front as a function of time. Finally, we test whether the simplified model can be calibrated to reproduce the depth of the wetting front over time obtained from the numerical simulations for the heterogeneous medium.

[28] Infiltration is represented by the Philip [1957] two-term infiltration model and redistribution by a rectangular drainage model [e.g., Jury and Horton, 2004]. The Philip model approximates an advancing wetting front in homogeneous soil as piston flow with a constant volumetric water content, θ_{wf} [$L^3 L^{-3}$], above the wetting front, and a uniform initial volumetric water content, θ_i [$L^3 L^{-3}$]. The depth of the wetting front, $z_{wf}(t)$ [L], as a function of the cumulative infiltration, $I(t)$ [L] at time t is

$$z_{wf}(t) = \frac{I(t)}{\theta_{wf} - \theta_i}. \quad (7)$$

The cumulative infiltration is defined as

$$I(t) = St^{\frac{1}{2}} + K_s t, \quad (8)$$

where the sorptivity, S [$L T^{-1.5}$], describes the capillarity of the soil.

[29] The rectangular drainage model simulates the advance of a wetting front during drainage as a function of elapsed time after infiltration ceases ($t > t_d$) assuming a uniform water content with depth above the wetting front, $\theta_{wf}(t)$, and a constant length of water (L) in the soil profile:

$$z_{wf} = L \frac{\theta_{wf}(t_d) - \theta_i}{\theta_{wf}(t) - \theta_i} \quad t > t_d. \quad (9)$$

[30] The model further assumes that the instantaneous drainage rate at the wetting front is equal to the gravity flux, $K(\theta_{wf})$. We assumed a power law relation between hydraulic conductivity and saturation [after Jury and Horton, 2004] and allow for nonzero initial water content:

$$\frac{K(\theta)}{K_s} = \left(\frac{\theta - \theta_i}{\theta_s - \theta_i} \right)^N, \quad (10)$$

where N [–] is the power law exponent. The water content of the draining layer as a function of time is

$$\theta_{wf}(t) = \left[\frac{NK_s}{L} (\theta_s - \theta_i)^{-(N+1)} (t - t_d) + \frac{1}{(\theta_s - \theta_i)^N} \right]^{\frac{-1}{N}} + \theta_i \quad t > t_d, \quad (11)$$

where $\theta_{wf}(t)$ is used to compute z_{wf} with (9). Using these models, the infiltration and drainage processes are described by five parameters (K_s , S , N , θ_s , and θ_i). These are the parameters we consider in the coupled and uncoupled hydrogeophysical inversion example.

[31] The utility of this analytical model for representing the movement of the wetting front during flow in a heterogeneous system was tested by calibrating the model to the observed wetting front depths simulated by the numerical model (Figure 3, diamonds). We used the DREAM [Vrugt *et al.*, 2008, 2009a] parameter estimation algorithm to select values of K_s , S , and N (Table 1) by minimizing the sum of squared residuals between the depth to the wetting front predicted by the analytical model versus those obtained from the numerical model, which explicitly includes heterogeneity. (Further details of the use of DREAM are provided in section 3.) The initial and saturated water content were set equal to those used in the heterogeneous

Table 1. Parameter Values Used to Generate the Error-Free Synthetic Data and Their Prior Uncertainty Ranges Used in the DREAM Inversion^a

Parameter	Synthetic Model Value	Parameter Range	
		Minimum	Maximum
K_s (m h ⁻¹)	0.010	0.001	0.1
S (m h ^{-0.5})	0.075	0.01	1
N	3.57	1.1	10
θ_i	0.17	0.01	0.5
θ_s	0.43	0.01	0.5
a (S m ⁻¹)	0.27	NE	NE
b	2.00	NE	NE
σ_i (S m ⁻¹)	-	0.0001	0.1
σ_{wf} (S m ⁻¹)	-	0.0001	0.1
z_{wf} (m)	-	0	100

^aNE means parameters not estimated. A dash means synthetic values were computed from the hydrologic model output using the petrophysical relation.

numerical model (Table 1) to provide consistent change in water content across the wetting front. As illustrated in Figure 3, the analytical model (solid line, no symbols) was able to replicate the depth of the wetting front observed in the heterogeneous soil very well. (The dashed lines are the 95% confidence interval for the prediction based on the simplified homogeneous model.) However, as is widely recognized, good calibration statistics do not guarantee that the model is a faithful representation of the system. For example, the calibrated analytical model may not make accurate predictions under different initial or boundary conditions. Furthermore, even for the conditions for which calibration was performed the analytical model was not able to replicate the water content behind the wetting front (compare Figures 2b and 2c). Of particular importance for electrical conductivity interpretation, the analytical model misrepresents the water content near the ground surface during drainage.

[32] The sharp wetting front and uniform water content above and below the wetting front simulated by the analytical water flow model results in a two-layer electrical conductivity distribution within the soil profile throughout infiltration and redistribution. The upper layer has an electrical conductivity associated with the water content above the wetting front, σ_{wf} , and extends from the ground surface to z_{wf} . The lower layer has an electrical conductivity associated with the initial water content, σ_i , and extends to infinite depth. This electrical conductivity structure allows the use of an analytical solution for the apparent conductivity measured with surface electrical conductivity over a horizontal layer [Telford et al., 1990]:

$$\sigma_a = \sigma_{wf} \left(1 + 4 \sum_{m=1}^{\infty} h^m \left(\left(1 + \left(\frac{2mz}{a} \right)^2 \right)^{-\frac{1}{2}} - \left(4 + \left(\frac{2mz}{a} \right)^2 \right)^{-\frac{1}{2}} \right) \right)^{-1}, \quad (12)$$

where a is the electrode spacing, z is the layer depth (equivalent to z_{wf} in this study), and $h = \frac{\sigma_{wf} - \sigma_i}{\sigma_{wf} + \sigma_i}$. The first fifty terms of the summation in (12) are evaluated. Using this analytical solution and the computationally less demanding analytical hydrologic model, the run time for the coupled

analytical models was reduced to approximately two seconds on a desktop computer (dual core 2.66 GHz processor with 4 GB memory), a time reduction of 1:3000 compared to the numerical model. It can be argued that similar computational conveniences often influence the selection of models for hydrologic interpretations.

2.3. Generating Synthetic ERT Data

[33] The synthetic experiment consisted of monitoring 5 days of infiltration followed by 15 days of redistribution. The true hydrologic and petrophysical model parameter values for each model are listed in Table 1. Synthetic data were simulated for 10 Wenner arrays (electrode spacings of 0.5, 1.0, 1.5, 2.0, 3.0, 4.0, 6.0, 8.0, 12, and 15 m). To generate the synthetic data sets, we calculated the water content profile at each measurement time ($t = \{2, 6, 12, 24, 36, 48, 72, 96, 120, 132, 144, 168, 192, 216, 240, 288, 336, 384, 480\}$ h) using the hydrologic models with the correct soil hydraulic parameters. We then converted the local water content values to electrical conductivities using the petrophysical relation and used these electrical conductivity profiles to calculate the apparent electrical conductivity values that would be measured with each electrode array at each measurement time. Finally, we added the same realization of uncorrelated, normally distributed, random noise with a mean of zero and a standard deviation of 2 mS m⁻¹ to each set of error-free apparent electrical conductivity values to mimic moderately noisy field data. Other options exist for corrupting the synthetic data, such as adding errors to the measured voltage; this topic will be considered in more detail in future investigations.

[34] One advantage of a synthetic experiment is that we can also produce ERT data that would have been measured if the simplified hydrologic model had been a true representation of the system. By using these data for inversion and comparing the results with inversions based on the “true” data described above, we can define the contributions of measurement error and model structural error to the inverse processes. Figure 4 shows the synthetic data sets with simulated measurement errors for three of the electrical resistivity arrays (electrode spacing of 0.5, 2.0, and 8.0m). The solid lines are the data derived from the numerical (heterogeneous) model and the dashed lines are the data derived from the analytical (homogeneous) model. These results suggest that even when the wetting front depths as a function of time match well with both the numerical and analytical models (Figures 2b and 2c) the corresponding electrical conductivity predictions can be significantly different due to the nonlinear sensitivity of electrical conductivity to changes in water content with depth. This suggests that model structural error is likely to be significant for our synthetic experiment. In practice, it would take considerable experience in hydrology and geophysics to predict the likely impacts of this model error on the hydrogeophysical inversion. But, by conducting a simple synthetic study, such as that shown here, a hydrologist and a geophysicist working together to build a coupled analysis framework could identify this shortcoming and design experiments and analyses appropriately.

3. Methods

[35] For each of the following examinations, we use synthetic electrical conductivity data to infer the hydrologic

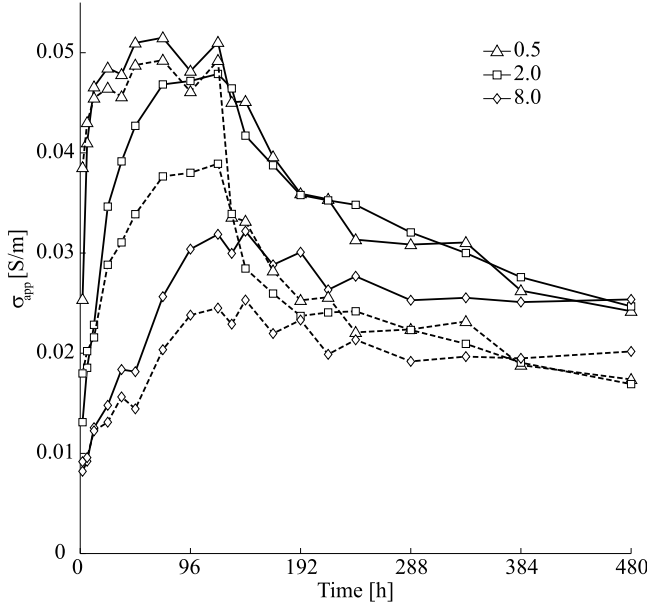


Figure 4. Subset of the synthetic apparent conductivity observations. Electrode spacings shown are 0.5, 2, and 8 m. The solid lines are from the numerical (heterogeneous) model, and the dashed lines are from the analytical (homogeneous) model.

parameter values of the calibrated analytical hydrologic model. We then use the predicted sets of parameter values to predict the wetting front depth through time. Finally, we characterize the maximum likelihood, (ML), prediction and its 95% confidence intervals using the DREAM inferred joint posterior probability density function of the parameters. In every case, we used the same inverse tools and settings for the coupled and uncoupled approaches and we provided the same information to both procedures.

3.1. Parameter Estimation Algorithm

[36] For all of our analyses, we use the recently developed DiffereNTial Evolution Adaptive Metropolis (DREAM) algorithm to sample the posterior pdf [Vrugt *et al.*, 2008, 2009a]. This method runs multiple Markov chains simultaneously for global exploration of the parameter space, and automatically tunes the scale and orientation of the proposal distribution en route to the posterior target pdf. The various chains are initialized at different starting points within the multidimensional hypercube defined in Table 1 (feasible parameter ranges), and learn from each other through a process of recombination and crossover. Standard convergence diagnostics of multiple chains are used to check whether the sampler has converged to the posterior distribution after 50,000 model evaluations. The DREAM sampling scheme is an extension of the SCEM-UA optimization algorithm [Vrugt *et al.*, 2003], but has the advantage of maintaining detailed balance and ergodicity and therefore provides an exact estimate of the posterior pdf.

3.2. Uncoupled Hydraulic Parameter Estimation

[37] We used DREAM to drive each of the three steps of an uncoupled inversion. In the first step, we used the DREAM algorithm to obtain sample realizations from the

posterior distribution of the geophysical parameter estimates. The posterior distribution $p(\mathbf{x}|\sigma_a)$ is the probability that the parameter set \mathbf{x} could occur given that the apparent conductivity values σ_a have been observed, where $\mathbf{x} = [\dots \sigma_{wf}(t_i), \sigma_i(t_i), z(t_i) \dots]$ such that $\sigma_{wf}(t_i)$ and $\sigma_i(t_i)$ are the conductivities above and below the wetting front located at depth z at time t_i and $\sigma_a = [\sigma_{1,1} \sigma_{1,2} \dots \sigma_{i,j} \dots \sigma_{n_t,n_s}]$ such that $\sigma_{i,j}$ is the apparent conductivity measured at array number j at time t_i . The total numbers of electrode arrays and observation times are given by n_s and n_t , respectively. Using Bayes' theorem, this probability is a function of a prior pdf, $p(\mathbf{x})$, for \mathbf{x} and the likelihood $p(\sigma_a|\mathbf{x})$, $p(\mathbf{x}|\sigma_a) = c p(\sigma_a|\mathbf{x}) p(\mathbf{x})$, where c is a normalizing constant. Because our geophysical model allows for simulation of $\sigma_a(t_i)$ from \mathbf{x} at any time t_i , i.e., $\hat{\sigma}_a(t_i) = f(\mathbf{x}(t_i))$, the likelihood describes the probability of misfit between simulated ($\hat{\sigma}_a$) and observed (σ_a) apparent conductivity values as a result of measurement or model errors. We use a classical Gaussian likelihood distribution that measures the distance between observed ($\hat{\sigma}_{i,j}$) and simulated apparent conductivity values, ($\sigma_{i,j}$):

$$p(\mathbf{x}|\sigma_a) = c \cdot p(\mathbf{x}) \prod_{i=1}^{n_t n_s} \frac{1}{\sqrt{2\pi\eta_{i,j}^2}} \exp\left(-\frac{(\hat{\sigma}_{i,j} - \sigma_{i,j})^2}{2\eta_{i,j}^2}\right). \quad (13)$$

Here, $\eta_{i,j}^2$ is the variance of the measurement error used to corrupt the synthetic data (η is used to denote variance to avoid confusion since standard nomenclature for both electrical conductivity and variance is σ). Note that $p(\mathbf{x})$ is chosen as being a noninformative prior using a uniform hypercube. It therefore cancels out of equation (13), and the posterior distribution is solely based on the misfit between measured and simulated apparent electrical conductivity values. The geophysical parameter ranges are listed in Table 1.

[38] In the second step of the uncoupled approach, geophysical parameter estimates are converted to hydrologic property estimates. The conductivity of the layers for each sample of \mathbf{x} drawn from $p(\mathbf{x}|\sigma)$ in the first step are converted to water content using a petrophysical relation such that the vectors θ_{wfs} , θ_i , and z_{wf} are the water content above and below the wetting front and the depth of the wetting front is z_{wf} as functions of time.

[39] In the third step of the uncoupled inversion, we use the hydrologic observations derived from geophysical measurements to constrain the hydrologic model parameters $\mathbf{m} = [K_s, S, N, \theta_s, \theta_i]$. We again use DREAM to sample the posterior distribution of the model parameters, but the data constraint is now provided by the inferred hydrologic data, which are obtained by assembling the maximum likelihood (ML) estimates of θ_{wfs} , θ_i and z_{wf} into a single measurement vector $\mathbf{y} = [\theta_{wfs}, \theta_i, z_{wf}]$ of length $3n_s n_t$. We define the measurement uncertainty for the elements of θ_{wfs} , θ_i , and z_{wf} (i.e., at each observation time) based on the standard deviation of the posterior pdfs estimated during the geophysical inversion step described above. We collect these uncertainties within a single vector ν . We use the following classical density function

$$p(\mathbf{m}|\mathbf{y}) = c \cdot p(\mathbf{m}) \prod_{i=1}^{3n_s n_t} \frac{1}{\sqrt{2\pi\nu_i^2}} \exp\left(-\frac{(\hat{y}_i - y_i)^2}{2\nu_i^2}\right), \quad (14)$$

where, ν_i^2 is the variance of each measurement error used to corrupt the synthetic data. The DREAM algorithm is then used

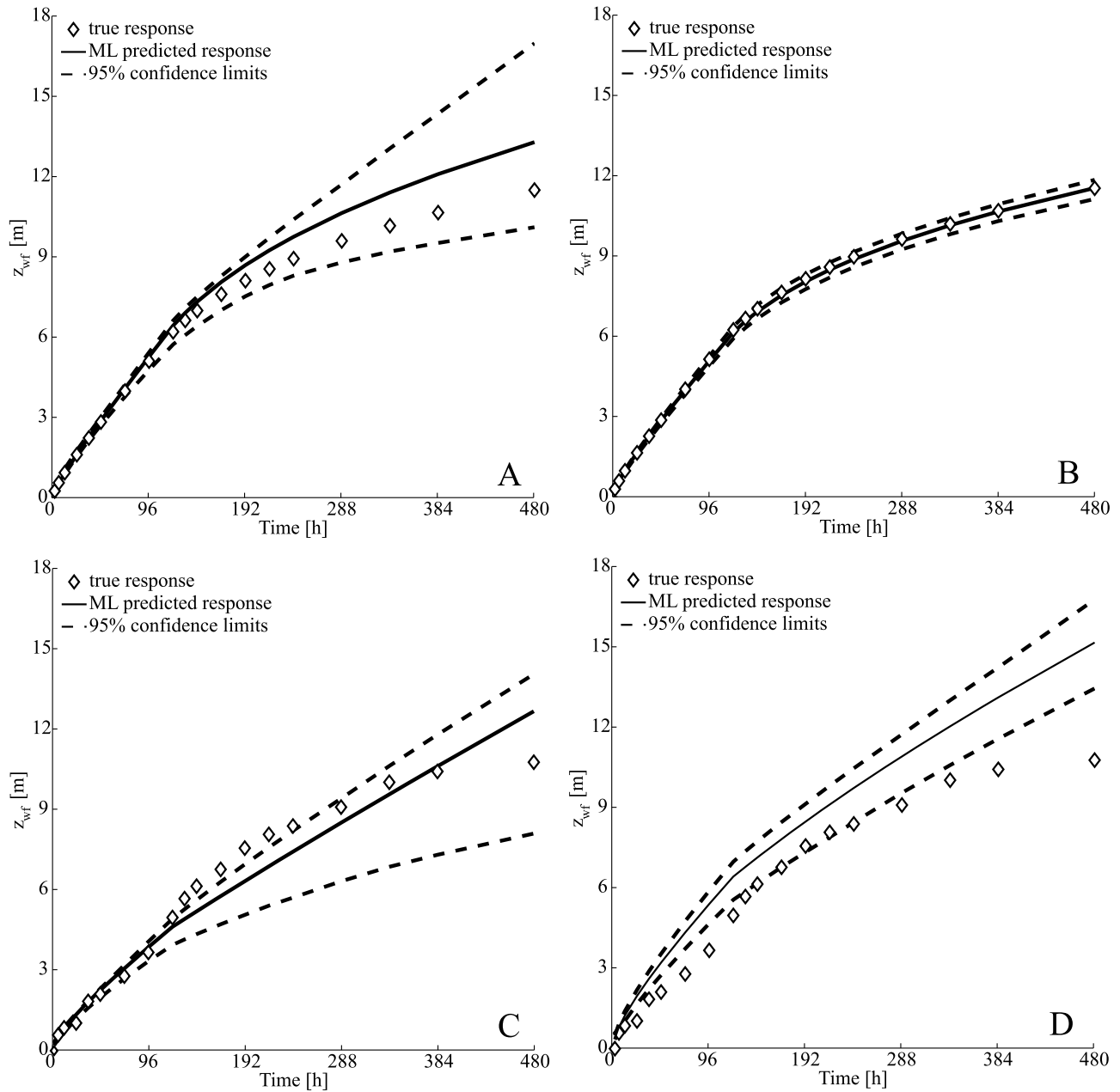


Figure 5. Predicted depth to wetting front for infiltration and redistribution. (a) Corrupted synthetic data generated using the analytical model. Uncoupled inversion completed with no model error (analytical model used in inversion). (b) Corrupted synthetic data generated using the analytical model. Coupled inversion completed with no model error (analytical model used in inversion). (c) Corrupted synthetic data generated using numerical (heterogeneous) model. Uncoupled inversion completed with the analytical model (model error). (d) Corrupted synthetic data generated using numerical (heterogeneous) model. Coupled inversion completed with the analytical model (model and measurement error).

to draw samples of $p(\mathbf{m}|\mathbf{y})$ starting with uniform prior ranges for each of the parameters as listed in Table 1. Note that equation (14) is identical to (13) with $\sigma_{i,j}$ replaced by y_i and \mathbf{x} replaced by \mathbf{m} . That is, we are treating the results of the geophysical inversion as if they were hydrologic observations. Uncertainty for each of the inferred hydrologic observations (θ_{wf} , θ_i and z_{wf}) was defined as the width of the posterior pdf carried over from the geophysical inversion for each measurement time. This “measurement” uncertainty is a combination of the impacts of the electrical conductivity

measurement error and the errors contributed by geophysical inversion. In contrast, if one of these properties were measured directly, (e.g., θ_{wf} with the gravimetric method), we could assign a measurement uncertainty based on the characteristics of the measurement method.

3.3. Coupled Hydraulic Parameter Estimation

[40] For the coupled approach, we did not determine the electrical conductivity structure at each observation time. Rather, we estimated the hydraulic model parameters $\mathbf{m} =$

Table 2. Maximum Likelihood Estimates and 95% Confidence Intervals of the Hydrologic Parameter Values Using the Uncoupled and Coupled Approaches Showing Measurement Error Only^a

Parameter	Synthetic Model Value	Uncoupled Analyses			Coupled Analyses		
		ML	95% Confidence		ML	95% Confidence	
			Lower	Upper		Lower	Upper
K_s (m h ⁻¹)	0.010	0.010	0.0074	0.013	0.0097	0.0091	0.010
S (m h ^{-0.5})	0.075	0.061	0.057	0.13	0.078	0.067	0.083
N	3.57	2.84	1.20	5.36	3.37	3.13	3.75
θ_i	0.17	0.18	0.13	0.20	0.17	0.17	0.18
θ_s	0.43	0.42	0.41	0.47	0.43	0.43	0.43

^aML, maximum likelihood.

$[K_s, S, N, \theta_s, \theta_i]$ directly from the apparent conductivity data (σ_a). We used the same density function as previously defined in equation (13) after replacing \mathbf{x} with \mathbf{m} , and DREAM was used to draw samples from the posterior pdf. Although not shown in this example, the coupled approach allows for simple inclusion of multiple measurement types because the misfit of each measurement can be weighted in the objective function based on the measurement uncertainty of that method. In other words, the objective function is defined in the measurement units and normalized by the measurement uncertainty for each measurement type.

4. Results

[41] Our numerical experiments were aimed at assessing the performance of coupled and uncoupled inversion for increasingly complicated model calibration scenarios. First, we compare the results of the two inversion strategies when measurement error is introduced, but no model structural error exists. Then, we evaluate the impact of model structural errors by calibrating a model for a homogeneous soil using data generated by a spatially heterogeneous medium.

4.1. Measurement Error Only, No Model Structural Inadequacies

[42] First, we conduct a hydrogeophysical inversion to assess the impacts of measurement error on the model calibration results. To do this, we use synthetic observations collected during infiltration that are based on the analytical hydrologic model with added measurement error. In this manner, the coupled and uncoupled inverse approaches use exactly the same hydrologic model and the underlying physical model correctly represents the hydrologic system under consideration. For these conditions, the uncoupled approach was able to simultaneously constrain the parameters K_s , S , θ_i , and θ_s with moderate uncertainty (Table 2). Yet, these parameter uncertainties propagate to large prediction errors (solid lines) and uncertainties (dashed lines) when compared to the true wetting front depth as a function of time (symbols) (Figure 5a). In contrast, the coupled approach recovers all of the parameters with very little uncertainty (Table 2). This results in predicted depths of the wetting front through time with relatively low error and low uncertainty (Figure 5b).

4.2. Measurement Error and Model Structural Inadequacies

[43] The uncoupled and coupled analyses were repeated using synthetic data generated for the heterogeneous soil

with the numerical hydrologic and geophysical models and added measurement error. In this case, however, the analytical models for a homogenous soil were used to interpret the results for both the coupled and uncoupled inversion schemes. Under these conditions, neither the coupled nor the uncoupled approach was able to produce predictions with low error and uncertainty (Figures 5c and 5d). In particular, both inversion approaches show large errors and/or uncertainties during redistribution. These errors arise due to the low water content region near the ground surface (Figure 2b) that is not captured in the analytical hydrologic model predictions (Figure 2c). This low water content, and therefore low electrical conductivity, region is located in a zone of high sensitivity of the electrical conductivity method [e.g., *Furman et al.*, 2003]. As a result, the analytical model has to reduce the water content behind the wetting front substantially to match the low apparent electrical conductivity that is caused by this shallow low water content region (Table 3).

5. Discussion and Conclusions

[44] We have presented a simple comparison of coupled and uncoupled hydrogeophysical inversion. The underlying premise of the coupled approach is that the interpretation of the geophysical measurements will be improved by using the hydrologic model to provide a context for interpretation. This advantage is demonstrated clearly by the improved accuracy and reduced uncertainty of the predictions of depth of the wetting front through time based on electrical conductivity measurements with measurement error when the hydrologic model was a good representation of the underlying physical system.

[45] There is, however, one caveat: regardless of the inverse approach used, if the hydrologic model does not represent the system adequately, then the interpretation will inherently be flawed. For the uncoupled approach, this hydrologic model error does not affect the geophysical interpretation. But, the hydrologic model error leads to errors when the geophysical results are used for calibration. For the coupled approach, the hydrologic model error provides a misleading context for interpreting the geophysical measurements. In general, it is likely that the value of coupled approach varies with the degree of hydrologic model conceptual error, although this has not been examined completely here. In some cases, such as shown here, the shortcomings of the hydrologic model may not impact the ability to make the hydrologic predictions of interest; but, they may impact the interpretation of the geophysical data using either the coupled or uncoupled approach. For example, in our case, the simplified hydro-

Table 3. Maximum Likelihood Estimates and 95% Confidence Intervals of the Hydrologic Parameter Values Using the Uncoupled and Coupled Approaches Showing Measurement and Model Error^a

Parameter	Uncoupled Analyses			Coupled Analyses		
	ML	95% Confidence		ML	95% Confidence	
		Lower	Upper		Lower	Upper
K_s (m h ⁻¹)	0.0038	0.0030	0.0077	0.0072	0.0055	0.0082
S (m h ^{-0.5})	0.055	0.042	0.093	0.15	0.085	0.15
N	1.69	1.11	2.73	1.48	1.11	1.95
θ_i	0.16	0.12	0.20	0.15	0.14	0.17
θ_s	0.35	0.32	0.43	0.38	0.38	0.39

^aML, maximum likelihood.

logic model could reproduce the prediction of interest well (the wetting front depth through time). But, the simplified model produced incorrect water content profiles at each time, which has a profound effect on the predicted electrical conductivity. In the end, our findings suggest that using a coupled hydrogeophysical inversion approach can greatly improve the value of geophysical measurements given an appropriate hydrologic model. But, the coupled approach cannot overcome fundamental limitations due to poor data, paucity of data, or model structural error.

[46] In addition to the direct advantages of coupled inversion for improved parameter estimation, we contend that the coupled approach has an additional, subtle advantage if a study involves a collaborative effort between a hydrologist and a geophysicist. Namely, because the coupled approach requires that the hydrologic and geophysical models be merged, it forces the hydrologist and the geophysicist to formulate a consistent framework for inference and solution. This is likely to support more complete sharing of supporting data and more extensive communication regarding the value of geophysical and other data as part of an integrating hydrogeophysical investigation. Yet, this may also be the primary limit to the routine implementation of coupled inversion. The formulation of common solution grids, time steps, and simulation accuracies requires an uncommon level of collaboration during scientific analysis.

[47] To us, the important general finding of this study is that there is a need for hydrologic insight and understanding when completing a hydrogeophysical study: no amount of additional geophysical data or improvements in joint or coupled inversion will overcome the limitations of a poor hydrologic conceptualization. On the other hand, this may also point to a role for uncoupled hydrogeophysical analysis: specifically, in many cases it may be worthwhile to conduct an independent geophysical survey as an initial step toward constructing a hydrologic conceptual model. This independent interpretation of the geophysical data may point out unexpected subsurface features that could alert a hydrologist to limitations in their conceptualization of the hydrologic processes.

[48] **Acknowledgments.** We would like to thank Kamini Singha and the anonymous reviewers for their thorough reviews and helpful suggestions for improving the manuscript. During this project, Andrew Hinnell was supported by the National Research Initiative of the USDA Cooperative State Research, Education and Extension Service, grant 2003-351023674. Ty Ferré was supported by the National Science Foundation as the director

of the CUAHSI HydroGeoPhysics facility under grant EAR 07-53521 awarded to the Consortium of Universities for the Advancement of Hydrologic Science. Jasper Vrugt was supported by a J. Robert Oppenheimer Fellowship from the Los Alamos National Laboratory postdoctoral program. J. A. Huisman is supported by grant HU1312/2 of the Deutsche Forschungsgemeinschaft (DFG). Michael Kowalsky was supported by the U.S. Department of Energy, contract DE-AC02-05CH11231.

References

- Archie, G. E. (1942), The electrical resistivity log as an aid in determining some reservoir characteristics, *Trans. Am. Inst. Min. Metall. Eng.*, **146**, 54–61.
- Binley, A., P. Winship, R. Middleton, M. Pokar, and J. West (2001), High-resolution characterization of vadose zone dynamics using cross-borehole radar, *Water Resour. Res.*, **37**(11), 2639–2652, doi:10.1029/2000WR000089.
- Binley, A., L. D. Slater, M. Fukes, and G. Cassiani (2005), Relationship between spectral induced polarization and hydraulic properties of saturated and unsaturated sandstone, *Water Resour. Res.*, **41**, W12417, doi:10.1029/2005WR004202.
- Carsel, R. F., and R. S. Parrish (1988), Developing joint probability distributions of soil water retention characteristics, *Water Resour. Res.*, **24**(5), 755–769, doi:10.1029/WR024i005p00755.
- Cassiani, G., G. Böhm, A. Vesnaver, and R. Nicolich (1998), A geostatistical framework for incorporating seismic tomography auxiliary data into hydraulic conductivity estimation, *J. Hydrol.*, **206**, 58–74, doi:10.1016/S0022694(98)00084-5.
- Cassiani, G., C. Strobbia, and L. Gallotti (2004), Vertical radar profiles for characterization of deep vadose zones, *Vadose Zone J.*, **3**, 1093–1105, doi:10.2113/3.4.1093.
- Cassiani, G., V. Bruno, A. Villa, N. Fusi, and A. Binley (2006), A saline trace test monitored via time-lapse surface electrical resistivity tomography, *J. Appl. Geophys.*, **59**, 244–256, doi:10.1016/j.jappgeo.2005.10.007.
- Chambers, J. E., O. Kuras, P. I. Meldrum, R. O. Ogilvy, and J. Hollands (2006), Electrical resistivity tomography applied to geologic, hydrogeologic and engineering investigations at a former waste-disposal site, *Geophysics*, **71**(6), doi:10.1190/1.2360184.
- Chen, J. S., S. Hubbard, Y. Rubin, C. Murray, E. Roden, and E. Majer (2004), Geochemical characterization using geophysical data and Markov chain Monte Carlo methods: A case study at the South Oyster bacterial transport site in Virginia, *Water Resour. Res.*, **40**, W12412, doi:10.1029/2003WR002883.
- Chen, J., S. Hubbard, J. Peterson, K. Williams, M. Fienen, P. Jardine, and D. Watson (2006), Development of a joint hydrogeophysical inversion approach and application to a contaminated fractured aquifer, *Water Resour. Res.*, **42**, W06425, doi:10.1029/2005WR004694.
- Daily, W., A. Ramirez, D. LaBrecque, and J. Nitao (1992), Electrical-resistivity tomography of vadose water movement, *Water Resour. Res.*, **28**(5), 1429–1442, doi:10.1029/91WR03087.
- Day-Lewis, F. D., J. M. Harris, and S. M. Gorelick (2002), Time-lapse inversion of crosswell radar data, *Geophysics*, **67**(6), 1740–1752, doi:10.1190/1.1527075.
- Day-Lewis, F. D., J. W. Lane Jr., J. M. Harris, and S. M. Gorelick (2003), Time-lapse imaging of saline-tracer transport in fractured rock using difference-attenuation radar tomography, *Water Resour. Res.*, **39**(10), 1290, doi:10.1029/2002WR001722.
- Day-Lewis, F. D., K. Singha, and A. Binley (2005), The application of petrophysical models to radar and electrical resistivity tomograms: Resolution-dependent limitations, *J. Geophys. Res.*, **110**, B08206, doi:10.1029/2004JB003569.
- Deiana, R., G. Cassiani, A. Villa, A. Bagliani, and V. Bruno (2008), Calibration of a vadose zone model using water injection monitored by GPR and electrical resistance tomography, *Vadose Zone J.*, **7**, 215–226, doi:10.2136/vzj2006.0137.
- Ferré, P. A., D. L. Rudolph, and R. G. Kachanoski (1996), Spatial averaging of water content by time domain reflectometry: Implications for twin rod probes with and without dielectric coatings, *Water Resour. Res.*, **32**(2), 271–279, doi:10.1029/95WR02576.
- Ferré, T., L. Bentley, A. Binley, N. Linde, A. Kemna, K. Singha, K. Holliger, J. A. Huisman, and B. Minsley (2009), Critical steps for the continuing advancement of hydrogeophysics, *Eos Trans. AGU*, **90**(23), 200, doi:10.1029/2009EO230004.

- Finsterle, S. A., and M. B. Kowalsky (2008), Joint hydrological-geophysical inversion for soil structure identification, *Vadose Zone J.*, 7, 287–293, doi:10.2136/vzj2006.0078.
- French, H., and A. Binley (2004), Snow melt infiltration: Monitoring temporal and spatial variability using time-lapse electrical resistivity, *J. Hydrol.*, 297, 174–186, doi:10.1016/j.jhydrol.2004.04.005.
- Furman, A., T. P. A. Ferré, and A. W. Warrick (2003), A sensitivity analysis of electrical resistivity tomography array types using analytical element modeling, *Vadose Zone J.*, 2, 416–423, doi:10.2113/2.3.416.
- Gallardo, L. A., and M. A. Meju (2003), Characterization of heterogeneous near-surface materials by joint 2D inversion of dc resistivity and seismic data, *Geophys. Res. Lett.*, 30(13), 1658, doi:10.1029/2003GL017370.
- Gallardo, L. A., and M. A. Meju (2004), Joint two-dimensional DC resistivity and seismic travel time inversion with cross-gradients constraints, *J. Geophys. Res.*, 109, B03311, doi:10.1029/2003JB002716.
- Hallihan, T., S. Paxton, I. Graham, T. Fenstemaker, and M. Riley (2005), Post-remediation evaluation of a LNAPL site using electrical resistivity imaging, *J. Environ. Monit.*, 7(4), 283–287, doi:10.1039/b416484a.
- Hillel, D. (1998), *Environmental Soil Physics*, Academic, San Diego, Calif.
- Hubbard, S. S., and Y. Rubin (2000), Hydrogeological parameter estimation using geophysical data: A review of selected techniques, *J. Contam. Hydrol.*, 45(1–2), 3–34, doi:10.1016/S0169-7722(00)00117-0.
- Hubbard, S. S., Y. Rubin, and E. Majer (1999), Spatial correlation structure estimation using geophysical and hydrogeological data, *Water Resour. Res.*, 35(6), 1809–1825, doi:10.1029/1999WR000040.
- Huisman, J. A., J. Rings, J. A. Vrugt, J. Sorg, and H. Vereecken (2010), Hydraulic properties of a model dike from coupled Bayesian and multi-criteria hydrogeophysical inversion, *J. Hydrol.*, 380, 62–73, doi:10.1016/j.jhydrol.2009.10.023.
- Hyndman, D. W., and S. M. Gorelick (1996), Estimating lithologic and transport properties in three dimensions using seismic and tracer data: The Kesterson aquifer, *Water Resour. Res.*, 32(9), 2659–2670, doi:10.1029/96WR01269.
- Hyndman, D. W., J. M. Harris, and S. M. Gorelick (1994), Coupled seismic and tracer test inversion for aquifer property characterization, *Water Resour. Res.*, 30(7), 1965–1977, doi:10.1029/94WR00950.
- Jury, W. A., and R. Horton (2004), *Soil Physics*, 6th ed., John Wiley, New York.
- Kemna, A., J. Vanderborght, B. Kulesa, and H. Vereecken (2002), Imaging and characterization of subsurface solute transport using electrical resistivity tomography (ERT) and equivalent transport models, *J. Hydrol.*, 267, 125–146, doi:10.1016/S0022694(02)00145-2.
- Kim, K., M. P. Anderson, and C. J. Bowser (1999), Model calibration with multiple targets: A case study, *Ground Water*, 37(3), 345–351, doi:10.1111/j.1745-6584.1999.tb01110.x.
- Klenke, J. M., and A. L. Flint (1991), Collimated neutron probe for soil-water content measurements, *Soil Sci. Am. J.*, 55(4), 916–923.
- Kowalsky, M. B., S. Finsterle, and Y. Rubin (2004), Estimating flow parameter distributions using ground-penetrating radar and hydrological measurements during transient flow in the vadose zone, *Adv. Water Resour.*, 27(6), 583–599, doi:10.1016/j.advwatres.2004.03.003.
- Kowalsky, M. B., S. Finsterle, J. Peterson, S. Hubbard, Y. Rubin, E. Majer, A. Ward, and G. Gee (2005), Estimation of field-scale soil hydraulic and dielectric parameters through joint inversion of GPR and hydrological data, *Water Resour. Res.*, 41, W11425, doi:10.1029/2005WR004237.
- Kowalsky, M. B., J. Birkholzer, J. Peterson, S. Finsterle, S. Mukhopadhyay, and Y. Tsang (2009), Sensitivity analysis for joint inversion of GPR and thermal-hydrological data from a large-scale underground heater test, *Nucl. Technol.*, 164(2), 169–179.
- Lambot, S., M. Antoine, I. van den Bosch, E. C. Slob, and M. Vanclooster (2004), Electromagnetic inversion of GPR signals and subsequent hydrodynamic inversion, *Vadose Zone J.*, 3, 1072–1081, doi:10.2113/3.4.1072.
- Lehikoinen, A., S. Finsterle, A. Voutilainen, M. B. Kowalsky, and J. P. Kaipio (2009), Dynamical inversion of geophysical ERT data: State estimation in the vadose zone, *Inverse Probl. Sci. Eng.*, 1, 1–22.
- Linde, N., A. Binley, A. Tryggvason, L. B. Pedersen, and A. Revil (2006a), Improved hydrogeophysical characterization using joint inversion of crosshole electrical resistance and ground penetrating radar traveltime data, *Water Resour. Res.*, 42, W12404, doi:10.1029/2006WR005131.
- Linde, N., S. Finsterle, and S. Hubbard (2006b), Inversion of tracer test data using tomographic constraints, *Water Resour. Res.*, 42, W04410, doi:10.1029/2004WR003806.
- Looms, M. C., A. Binley, K. H. Jensen, L. Nielsen, and T. M. Hansen (2008a), Identifying unsaturated hydraulic parameters using an integrated data fusion approach on cross-borehole geophysical data, *Vadose Zone J.*, 7, 238–248, doi:10.2136/vzj2007.0087.
- Looms, M. C., K. H. Jensen, A. Binley, and L. Nielsen (2008b), Monitoring unsaturated flow and transport using cross-borehole geophysical methods, *Vadose Zone J.*, 7, 227–237, doi:10.2136/vzj2006.0129.
- Menke, W. (1984), *Geophysical Data Analysis: Discrete Inverse Theory*, Elsevier, New York.
- Moysey, S., K. Singha, and R. Knight (2005), A framework for inferring field-scale rock physics relationships through numerical simulation, *Geophys. Res. Lett.*, 32, L08304, doi:10.1029/2004GL022152.
- Moysey, S., R. J. Knight, and K. Singha (2006), Relating geophysical and hydrologic properties using field-scale rock physics, in *Proceedings of the 16th International Conference on Computational Methods in Water Resources, Denmark, 19–22 June*, edited by P. J. Binning et al., pp. 1–8, Tech. Univ. of Denmark, Lyngby, Denmark. (Available at <http://proceedings.cmrw-xvi.org/conferenceDisplay.py?confId=a051>)
- Mualem, Y. (1976), New model for predicting hydraulic conductivity of unsaturated porous media, *Water Resour. Res.*, 12(3), 513–522, doi:10.1029/WR012i003p00513.
- Mugunthan, P., and C. A. Shoemaker (2006), Assessing the impacts of parameter uncertainty for computationally expensive groundwater models, *Water Resour. Res.*, 42, W10428, doi:10.1029/2005WR004640.
- National Academy of Sciences (2000), *Seeing Into the Earth: Noninvasive Characterization of the Shallow Subsurface for Environmental and Engineering Applications*, 129 pp., Natl. Acad. Press, Washington, D. C.
- Neuman, S. P. (2003), Maximum likelihood Bayesian averaging of uncertain model predictions, *Stochastic Environ. Res. Risk Assess.*, 17(5), 291–305, doi:10.1007/s00477-003-0151-7.
- Neuman, S. P., P. J. Wierenga, and T. J. Nicholson (2003), A comprehensive strategy of hydrogeologic modeling and uncertainty analysis for nuclear facilities and sites, *Rep. NUREG/CR-6805*, U.S. Nucl. Regul. Comm., Washington, D. C.
- Park, S. (1998), Fluid migration in the vadose zone from 3-D inversion of resistivity monitoring data, *Geophysics*, 63(1), 41–51, doi:10.1190/1.1444326.
- Philip, J. R. (1957), The theory of infiltration: 4. Sorptivity and algebraic infiltration equations, *Soil Sci.*, 84(3), 257–264, doi:10.1097/0001069495709000-00010.
- Poeter, E. P., and M. C. Hill (1999), UCODE, a computer code for universal inverse modeling, *Comput. Geosci.*, 23(4), 457–462, doi:10.1016/S0098-3004(98)00149-6.
- Rucker, D. F., and T. P. A. Ferré (2004), Parameter estimation for soil hydraulic properties using zero-offset borehole radar: Analytical method, *Soil Sci. Soc. Am. J.*, 68, 1560–1567.
- Sandberg, S. K., L. D. Slater, and R. Versteeg (2002), An integrated geophysical investigation of the hydrogeology of an anisotropic unconfined aquifer, *J. Hydrol.*, 267, 227–243, doi:10.1016/S0022694(02)00153.
- Sicilia, G. T., and S. M. Moysey (2007), Comparison of hydrologic parameter estimates using sequential and integrated data fusion during a GPR monitored infiltration event, *Eos Trans. AGU*, 88(52), Fall Meet. Suppl., Abstract H23A016.
- Simunek, J., M. Sejna, and M. T. van Genuchten (1999), The HYDRUSD software package for simulating two-dimensional movement of water, heat, and multiple solutes in variably saturated media, version 2.0, *Rep. IGWMC-TPS-53*, 251 pp., Int. Ground Water Modeling Cent., Colo. Sch. of Mines, Golden.
- Singha, K., and S. Moysey (2006), Accounting for spatially variable resolution in electrical resistivity tomography through field-scale rock physics relations, *Geophysics*, 71(4), A25–A28, doi:10.1190/1.2209753.
- Slater, L. (2007), Near surface electrical characterization of hydraulic conductivity: From petrophysical properties to aquifer geometries—A review, *Surv. Geophys.*, 28, 169–197, doi:10.1007/s10712-007-9022-y.
- Telford, W. M., L. P. Geldart, and R. E. Sheriff (1990), *Applied Geophysics*, 2nd ed., Cambridge Univ. Press, Cambridge, U. K.
- Topp, G. C., J. L. Davis, and A. P. Annan (1980), Electromagnetic determination of soil-water content: Measurements in coaxial transmission lines, *Water Resour. Res.*, 16(3), 574–582, doi:10.1029/WR016i003p00574.
- Troldborg, L., J. C. Refsgaard, K. H. Jensen, and P. Engesgaard (2007), The importance of alternative conceptual models for simulation of concentrations in a multi-aquifer system, *Hydrogeol. J.*, 15, 843–860, doi:10.1007/s10040-007-0192-y.
- Turesson, A. (2006), Water content and porosity estimated from ground-penetrating radar and resistivity, *J. Appl. Geophys.*, 58, 99–111, doi:10.1016/j.jappgeo.2005.04.004.
- Vanderborght, J., A. Kemna, H. Haddad, and H. Vereecken (2005), Potential of electrical resistivity tomography to infer aquifer transport characteristics from tracer studies: A synthetic case study, *Water Resour. Res.*, 41, W06013, doi:10.1029/2004WR003774.

- van Genuchten, M. T. (1980), A closed-form equation for predicting the hydraulic conductivity of unsaturated soils, *Soil Sci. Soc. Am. J.*, *44*(5), 892–898.
- Vereecken, H., S. Hubbard, A. Binley, and T. Ferré (2004), Hydrogeophysics: An introduction from the guest editors, *Vadose Zone J.*, *3*, 1060–1062, doi:10.2113/3.4.1060.
- Vozoff, K., and D. L. B. Jupp (1975), Joint inversion of geophysical data, *Geophys. J. R. Astron. Soc.*, *43*(3), 977–991.
- Vrugt, J. A., and B. A. Robinson (2007), Treatment of uncertainty using ensemble methods: Comparison of sequential data assimilation and Bayesian model averaging, *Water Resour. Res.*, *43*, W01411, doi:10.1029/2005WR004838.
- Vrugt, J. A., H. V. Gupta, W. Bouten, and S. Sorooshian (2003), A shuffled complex evolution Metropolis algorithm for optimization and uncertainty assessment of hydrologic model parameters, *Water Resour. Res.*, *39*(8), 1201, doi:10.1029/2002WR001642.
- Vrugt, J. A., C. J. F. ter Braak, M. P. Clark, J. M. Hyman, and B. A. Robinson (2008), Treatment of input uncertainty in hydrologic modeling: Doing hydrology backward with Markov chain Monte Carlo simulation, *Water Resour. Res.*, *44*, W00B09, doi:10.1029/2007WR006720.
- Vrugt, J. A., C. J. F. ter Braak, C. G. H. Diks, D. Higdon, B. A. Robinson, and J. M. Hyman (2009a), Accelerating Markov chain Monte Carlo simulation by differential evolution with self-adaptive randomized subspace sampling, *Int. J. Nonlinear Sci. Numer. Simul.*, *10*(3), 273–290.
- Vrugt, J. A., B. A. Robinson, and J. M. Hyman (2009b), Self-adaptive multi-method search for global optimization in real-parameter spaces, *IEEE Trans. Evol. Comput.*, *13*(2), 243–259, doi:10.1109/TEVC.2008.924428.
- Ye, M., S. P. Neuman, and P. D. Meyer (2004), Maximum likelihood Bayesian averaging of spatial variability models in unsaturated fractured tuff, *Water Resour. Res.*, *40*, W05113, doi:10.1029/2003WR002557.
- Yeh, T.-C. J., S. Liu, R. J. Glass, K. Baker, J. R. Brainard, D. Alumbaugh, and D. LaBrecque (2002), A geostatistically based inverse model for electrical resistivity surveys and its applications to vadose zone hydrology, *Water Resour. Res.*, *38*(12), 1278, doi:10.1029/2001WR001204.

T. P. A. Ferré and A. C. Hinnell, Hydrology and Water Resources, University of Arizona, Tucson, AZ 85721-0011, USA. (andrew.hinnell@gmail.com)

J. A. Huisman and J. Rings, ICG 4 Agrosphere, Forschungszentrum Jülich, D-52425 Jülich, Germany.

M. B. Kowalsky, Earth Sciences Division, Lawrence Berkeley National Laboratory, Berkeley, CA 94720, USA.

S. Moysey, Environmental Engineering and Earth Sciences, Clemson University, Clemson, SC 29634, USA.

J. A. Vrugt, Center for Nonlinear Studies, Mail Stop B258, Los Alamos, NM 87545, USA.